Sensors and Actuators B 162 (2012) 284–291

Contents lists available at SciVerse ScienceDirect

Sensors and Actuators B: Chemical

journal homepage: www.elsevier.com/locate/snb

Mathematical modeling and experimental results of a sandwich-type amperometric biosensor

Marcelo Ricardo Romero, Ana M. Baruzzi, Fernando Garay*

INFIQC, Dpto. de Físico Química, Facultad de Ciencias Químicas, UNC, Pab. Argentina, ala 1, 2° piso, Ciudad Universitaria, 5000 Córdoba, Argentina

ARTICLE INFO

Article history:
Received 13 October 2011
Received in revised form
21 December 2011
Accepted 22 December 2011
Available online 29 December 2011

Keywords:
Ping-pong
Amperometric sensor
Finite difference
Sandwich-type biosensor
Lactate
Hydrogel
Oxidase

ABSTRACT

A comprehensive numerical treatment of the diffusion and reaction within a sandwich-type amperometric biosensor is presented. The model considers that the enzyme reacts according to a ping-pong mechanism and that it is entrapped into a so-called enzymatic matrix placed between two diffusion membranes. It is found that the concentrations of reagents and products within the sensor are difficult of being compared to those of the bulk. In this regard, the use of approximate analytical solutions would involve errors in the analysis of kinetic parameters corresponding to this kind of biosensors. Provided the mediator species are in high concentration or diffuse much faster than the substrate, the response time of a biosensor of this kind would be determined by the diffusion of the substrate though the external membrane. In this sense, those systems with immobilized mediators, in which diffusion of electrons or holes is assumed for the charge transport process, could be also described by this model. Thus, the thickness and the permeability to the analyte of the external membrane are critical parameters for improving the response time of a sandwich-type biosensor.

The simulated curves are compared with experimental profiles corresponding to a lactate amperometric biosensor obtaining consistent results. In a future publication a non-linear fitting algorithm will be combined to the model for the extraction of kinetic and/or geometric parameters.

1. Introduction

Amperometric enzyme-based biosensors are devices that have shown to be extremely useful for monitoring and quantifying wide variety of substances related to clinical, environmental and food samples [1–8]. The success of an amperometric biosensor particularly depends on the strategy for immobilizing the enzyme at the surface of an electrode [1,3,4,6,7]. A simple approach that has been widely used corresponds to the so-called sandwich-type amperometric biosensors [3,4,9–11]. These devices are based on trapping the enzyme between two membranes that, at the same time, serve for the diffusion-controlled transport of species and the rejection of potential interferences [9,10]. The general situation of a sandwich-type amperometric biosensor is schematized in Fig. 1.

There are different strategies for immobilizing the enzyme between the two polymeric membranes. In all cases, the enzyme is physically or chemically linked to a given matrix or composite, the enzymatic matrix (E-matrix), that would ensure the stability of the enzyme and improve the performance of a given biosensor [1,6]. Thus, the sensor has the shape of a sandwich where the two diffusion membranes entrap the enzymatic matrix [3,4,11]. The convection movement of the electrolyte stops at the outer membrane, while the flow of reagents and products is controlled by diffusion within the sensor (Fig. 1). In this work, it is assumed that the enzyme is an oxidase that catalyzes the oxidation of a substrate (S) and the reduction of the mediator (M) according to a conventional ping-pong mechanism [11–18].

Even though the mediator could be any species that involve a reversible redox couple, oxygen was selected simply because it is the natural mediator of most oxidases and several enzymatic constants are available for ping-pong reactions with this reagent [1,2,11,18]. Besides, the concentration of oxygen in aqueous solutions or blood is well-known, it is present in most real samples, it is free, and it is more stable and diffuses much faster than the other involved species (which is an important advantage over other mediators) [1]. Although both products of the enzymatic reaction can diffuse within and without the sensor, only the species (P) is considered to be electroactive. The reactions occurring in the enzymatic membrane can be summarized as:

$$E_r + S \underset{k_{-1}}{\overset{k_1}{\rightleftarrows}} E_rS \xrightarrow{k_2} E_o + R \quad (1)$$

$$E_o + M \underset{k_{-3}}{\overset{k_3}{\rightleftarrows}} E_oM \xrightarrow{k_4} E_r + P \quad (2)$$

* Corresponding author. Tel.: +54 351 4334169/80; fax: +54 351 4334188.
E-mail addresses: fgaray@fcq.unc.edu.ar, fsgaray@gmail.com (F. Garay).

0925-4005/$ – see front matter © 2012 Elsevier B.V. All rights reserved.
doi:10.1016/j.snb.2011.12.079

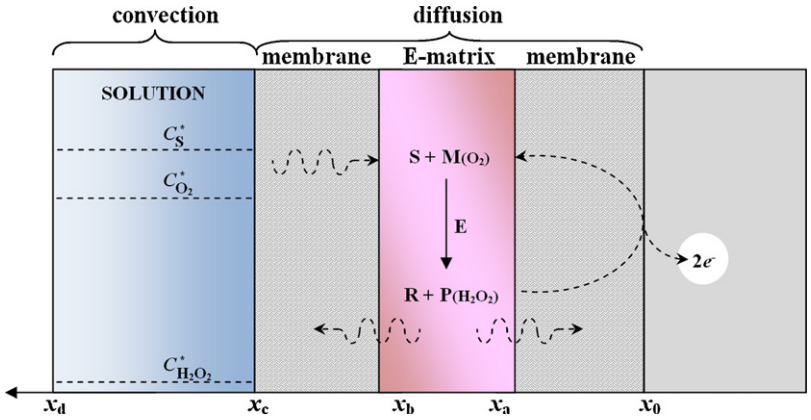

Fig. 1. Scheme of a sandwich-type amperometric biosensor.

where E_r and E_o are the reduced and oxidized forms of the enzyme while E_rS and E_oM are the intermediate complexes of the enzyme with substrate and mediator, respectively. The following reaction takes place at the electrode surface:

$$P \xrightarrow{-2e^-} M \tag{3}$$

In this way, the oxidation of the enzymatic product P electrochemically regenerates the species M. Species P and M may be replaced by H_2O_2/O_2, or by any other redox couple in which organic, inorganic, or metal–organic complexes that usually involve cations of Fe, Ru or Os mediate the transfer of charge between the enzyme and the electrode [1,2,11,17,18]. The main objective of adding artificial mediators is to increase the concentration of M (C_M) and to lower the potential applied to the working electrode [1,2]. The latter diminishes the effect of interfering species that are electrochemically active when the applied potential is around 0.6 V versus Ag|AgCl. For the case of sandwich-type amperometric biosensors, however, other strategies such as the chemical modification of the inner and/or the outer membranes can be used to minimize the effect of interfering species [1,3,9,11].

For the analysis of reactions (1) and (2) it is necessary to consider the concentration of species into the E-matrix. Moreover, the concentration of reagents and enzymatic products can vary according to their position from the electrode. As a consequence, the complex interplay of diffusion and kinetic contributions provides amperometric signals that cannot be described by an analytical expression [17]. In this regard, approximate solutions can rarely be used since the boundary conditions of most systems change from a limiting situation to another while a calibration curve is carried out [17,19]. On the contrary, numerical simulation can be applied not only to calculate the response of a biosensor over a wide range of experimental parameters, but also to get an insight about the concentration profiles of involved species within the film [17,19,20]. For these reasons, numerical techniques have been used to describe the transients and the steady-state situations of numerous biosensors related to diverse boundary conditions [17,20–29].

In this work, a simple and comprehensive numerical algorithm is provided to solve the coupled non-linear kinetic-diffusion problem of a sandwich-type amperometric biosensor. The model considers that the enzymatic reaction takes place according to a ping-pong mechanism, which would be the case for most oxidase-type enzymes [13,14,18]. Taking into account that most sandwich-type biosensors have thicknesses that go between 10 and 100 μm, this simple explicit algorithm would be an effortless and fast enough way to describe the responses as well as the concentration profiles associated with amperometric sensors of this kind [28]. More complicated mathematical approaches should be used for the case of biosensors of nanometric thickness [17]. With a better understanding of the several variables that affect a sensor of this kind, it would be easier to explain experimental effects such as the lack of linearity of a calibration curve. Finally, simulated results are compared with experimental data corresponding to a sandwich-type lactate biosensor.

2. The model

For the development of a theoretical model that describes an enzymatic biosensor based on the scheme of Fig. 1 it was assumed that:

- The enzyme is present only in the E-matrix and has a constant concentration value (C_E).
- For $t = 0$, the concentration of M (C_M) is a constant and the concentration of S (C_S) and P (C_P) is equal to zero in the sensor and the solution.
- Within the sensor, the diffusion coefficient of every involved species is constant and the enzyme cannot move since it has been cross-linked with the E-matrix.
- The enzymatic product P can be rapidly re-oxidized at the electrode surface, thus $(C_P)_{x=0} = 0$.
- The thickness of the biosensor (Δx) would be between 10 and 100 μm, which is a typical thickness for sandwich-type biosensors [11,27]. Thinner or thicker films would require either longer calculation times or a better calculation mesh [17]. However, since the result can be obtained within 10 s, we prefer the simplicity of this explicit algorithm [28].
- The concentration of background electrolyte is high enough to neglect effects associated with the migration of species [29,30].

From the analysis of Eqs. (1) and (2) it is possible to obtain the following expression:

$$v = \frac{v_{max}}{1 + K_S/C_S + K_M/C_M} \tag{4}$$

where $v_{max} = C_E k_2 k_4 [(k_2 + k_4)]^{-1} = C_E k_{cat}$, $K_S = k_4(k_{-1} + k_2)[(k_2 + k_4)k_1]^{-1}$, $K_M = k_2(k_{-3} + k_4)[(k_2 + k_4)k_3]^{-1}$, while K_S and K_M are usually called the Michaelis constants for S and M, respectively. If there is linear mass transfer along the x-axis that is normal to the electrode surface, then the diffusion of species within the membranes, i.e. $\forall x/(x_c \geq x > x_b)\text{^}(x_a \geq x > x_0)$ can be described by the following set of equations:

$$\frac{\partial C_S}{\partial t} = D_S \frac{\partial^2 C_S}{\partial x^2} \tag{5}$$

$$\frac{\partial C_M}{\partial t} = D_M \frac{\partial^2 C_M}{\partial x^2} \quad (6)$$

$$\frac{\partial C_P}{\partial t} = D_P \frac{\partial^2 C_P}{\partial x^2} \quad (7)$$

$$\frac{\partial C_R}{\partial t} = D_R \frac{\partial^2 C_R}{\partial x^2} \quad (8)$$

where D_S, D_M, D_P, and D_R are the respective diffusion coefficients for the species within the membrane. The following equations are used to consider the reactions at the enzymatic matrix, i.e. $\forall x/(x_b \geq x > x_a)$:

$$\frac{\partial C_S}{\partial t} = D_S \frac{\partial^2 C_S}{\partial x^2} - \frac{v_{max}}{1 + K_S/C_S + K_M/C_M} \quad (9)$$

$$\frac{\partial C_M}{\partial t} = D_M \frac{\partial^2 C_M}{\partial x^2} - \frac{v_{max}}{1 + K_S/C_S + K_M/C_M} \quad (10)$$

$$\frac{\partial C_P}{\partial t} = D_P \frac{\partial^2 C_P}{\partial x^2} + \frac{v_{max}}{1 + K_S/C_S + K_M/C_M} \quad (11)$$

$$\frac{\partial C_R}{\partial t} = D_R \frac{\partial^2 C_R}{\partial x^2} + \frac{v_{max}}{1 + K_S/C_S + K_M/C_M} \quad (12)$$

Finally, the flux of species at the electrode surface is described by:

$$\frac{I(t)}{n_e F A} = -D_P \left(\frac{\partial C_P}{\partial x}\right)_{x=0} = D_M \left(\frac{\partial C_M}{\partial x}\right)_{x=0} \quad (13)$$

$$\left(\frac{\partial C_S}{\partial x}\right)_{x=0} = \left(\frac{\partial C_R}{\partial x}\right)_{x=0} = 0 \quad (14)$$

To evaluate concentration profiles and the respective outcomes of the model Eqs. (5)–(14) are reformulated according to the following finite difference expressions:

For $x/(x_c \geq x > x_b)\wedge(x_a \geq x > x_0)$:

$$(C_i)_j^{t+1} = (C_i)_j^t + \frac{D_i \Delta t}{\Delta x^2}[(C_i)_{j-1}^t - 2(C_i)_j^t + (C_i)_{j+1}^t] \quad (15)$$

For $x/(x_b \geq x > x_a)$:

$$(C_i)_j^{t+1} = (C_i)_j^t + \frac{D_i \Delta t}{\Delta x^2}[(C_i)_{j-1}^t - 2(C_i)_j^t + (C_i)_{j+1}^t] \pm \frac{v_{max}}{1 + K_S/(C_S)_j^t + K_M/(C_M)_j^t} \quad (16)$$

where the sign minus is applied to solve Eqs. (9) and (10) while the sign plus is used for the case of Eqs. (11) and (12). The subindex i represents a given species, while j corresponds to a given position within the membrane [28]. For $x = 0$:

$$\Psi(t) = \frac{I(t)}{n_e F A C_S^*}\frac{t}{\Delta x} = \frac{D_P \Delta t N}{\Delta x^2}\frac{(C_P)_1^t}{C_S^*} \quad (17)$$

In the last expression, $\Psi(t)$ corresponds to the dimensionless current at the time $t = N\Delta t$. The dimensionless diffusion of the mediator was fixed as: $D_M \Delta t/\Delta x^2 = 0.45$ [28]. Eqs. (15)–(17) provide the theoretical transients from which steady-state currents can be extracted.

3. Experimental

3.1. Reagents

All solutions were prepared with ultra pure water (18 M cm^{-1}) from a Millipore Milli-Q system. The base electrolyte solution (0.1 M) consisted in 0.05 M HK_2PO_4/0.05 M H_2KPO_4 (Merck, Germany). This solution was renewed weekly and small amounts of H_2SO_4 (Baker, USA) or KOH (Merck, Germany) were used to fix it at pH 7.0. Stock solutions of 0.1 M lactate (Sigma, USA) and 5% (v/v) glutaraldehyde (Backer, USA) were prepared in the base electrolyte. A total amount of 100 U LOD from *Pediococcus* species (Sigma, USA) was dissolved in 1000 μL of base electrolyte. Then, the solution was separated into aliquots of 20 μL and stored at −20 °C. Thus, every aliquot bears 2 U of LOD. Mucin (Sigma, USA) was mortared and stored as dry powder at 4 °C. Bovine serum albumin (Sigma, USA) was used as received. All solutions were stored at 4 °C. All reagents were of analytical grade and used as received. Polycarbonate membranes of 0.05 μm pore size were cut in discs of 6 mm diameter (Millipore, USA).

3.2. Apparatus

All electrochemical experiments were performed with an Autolab PGSTAT 30 Electrochemical Analyzer (Eco Chemie, The Netherlands). The measurements were carried out using a conventional three-electrode system. The working electrode was a homemade 2 mm diameter Pt disc, while a Pt wire was the counter electrode, and a Ag|AgCl|KCl (3 M) (CH Instruments, USA) was the reference electrode. Amperometric detection was carried out under batch conditions and the solution was stirred at 120 rpm during the whole electrochemical experiment.

3.3. Construction of the enzymatic electrode

In this work the strategy for preparing the enzymatic LOD-matrix is the same as that described previously [11]. Shortly, 6.0 mg of a mixture 70/30 mucin/albumin was dissolved in 40 μL of base electrolyte and then transferred into a vial containing 2 U of LOD. Each enzymatic electrode was prepared using an aliquot of 6 μL LOD-matrix mixed with 3 μL of glutaraldehyde. The resulting hydrogel was entrapped between two membranes of polycarbonate. After waiting for 5 min, buffer solution was used to rinse the electrode and eliminate glutaraldehyde molecules that did not react in the E-matrix.

3.4. Calculations

All calculations were performed in Fortran 77 with an Intel Visual Fortran Compiler for Microsoft Visual Studio 2008. The time required for each simulated curve was around 5 s when a laptop with an Intel Core i3 processor of 330 MHz was used.

4. Results and discussion

Considering that Eq. (3) takes place when a platinum working electrode is kept at 0.65 V, the enzymatic product H_2O_2 can be rapidly re-oxidized at the electrode surface, and its concentration at $x = 0$ will be zero during the whole experiment [31,32]. In other words, Nernst equation is considered at the electrode surface and the electrochemical reaction is limited by the diffusion of H_2O_2 at any time. Within the sensor, the diffusion coefficient of every involved species is considered constant. Besides, the diffusion coefficients of H_2O_2 and O_2 are the highest when compared with the other species. The enzyme cannot move since it has been cross-linked with the E-matrix. The solution and the sensor are saturated with O_2 prior to the beginning of the experiment, while S is added to the solution at $t = 0$. Although the thickness of the biosensor (Δx) could take practically any value in the theory, most real sandwich-type biosensors are between 10 and 100 μm thick [11,27]. The thicknesses of the membranes and the E-matrix can be changed. In this opportunity, however, it is assumed a sandwich-type biosensor with $\Delta x = 100$ μm where the membranes and the

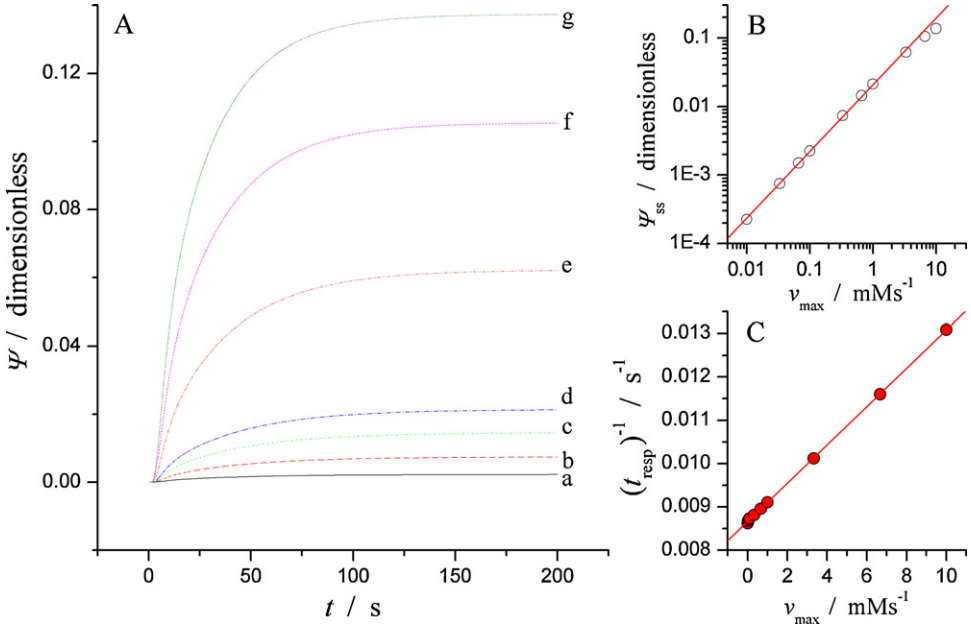

Fig. 2. (A) Transients of Ψ–t calculated for: C_S = 0.1 mM, C_M = 0.274 mM, $D_S = 1 \times 10^{-6}$ cm^2 s^{-1}, $D_P = 5 \times 10^{-6}$ cm^2 s^{-1}, $D_M = 1 \times 10^{-5}$ cm^2 s^{-1}, $K_M = 7.1 \times 10^{-5}$ M, $K_S = 2.2 \times 10^{-2}$ M, Δx = 100 μm, δt = 40 ms, and different values of v_{max} (mM s^{-1}): (a) 0.010, (b) 0.033, (c) 0.066, (d) 0.10, (e) 0.33, (f) 0.66, (g) 1.0, (h) 3.3, (i) 6.6, (j) 10. (B) Dependence of Ψ_{ss} on v_{max}. (C) Dependence of $(t_{resp})^{-1}$ on v_{max}.

enzymatic matrix have the same thickness 33 μm. In a future publication, a non-linear fitting algorithm will be implemented to fit a set of experimental curves and estimate the actual thickness of these layers [17,33,34].

All simulated curves are presented (or analyzed) against dimensioned variables. It is expected that the discussion and conclusions can be easily understood in this way.

Typical transients of the dimensionless current as function of time calculated for different values of v_{max} are shown in Fig. 2A. For those calculations, the values of K_M and K_S corresponding to the enzyme lactate oxidase (LOD) exposed to O_2 and D-lactate have been used, respectively [14]. It was also considered that C_M = 0.274 mM, which is the saturated oxygen concentration in blood [35]. As stated above, a thickness of 33 μm has been considered for the diffusion membranes and the enzymatic matrix of this sandwich-type biosensor.

The different profiles clearly exhibit an increase of Ψ when the value of v_{max} is raised. Actually, provided $v_{max} < 3$ mM s^{-1}, linear behavior is observed for the dependence of the dimensionless steady-state current (Ψ_{ss}) on v_{max}. When v_{max} is too high the last term of Eq. (16) competes with the term corresponding to the diffusion of S and/or M, resulting in lower current than expected. In other words, the diffusion of S and/or M is not high enough to keep the entire amount of enzyme working in the sensor.

Fig. 2C shows that the concentration of the enzyme in the sandwich can be linearly related to the reciprocal of the response time (t_{resp}) determined when the signal reaches the 95% of Ψ_{ss}. This outcome cannot be easily explained since it is rather difficult to measure the concentration of O_2 within the enzymatic matrix or in the inner membrane. Csóka et al. found that O_2 would be totally depleted if this molecule would diffuse through an enzymatic membrane of 200 μm [36]. Nevertheless, their experimental setup did not involve the regeneration of O_2 at the working electrode.

From Eqs. (1) and (2) it is easy to conclude that the mediator is being consumed at the enzymatic membrane, and its consumption may compromise the velocity of the enzymatic reaction. However, for the case of an electrochemical biosensor, the product is oxidized at the electrode surface and generates back the mediator. Thus, the consumption of the mediator will be relevant for the enzymatic reaction depending not only on the value of C_M, but also on the diffusion coefficients of P and M. The rapid diffusion of these species through the sandwich minimizes the concentration changes of M at the E-matrix.

Fig. 3 shows the dependence of the concentration of S, P and M on the distance from the electrode surface and on the time elapsed after the addition of S. These concentration profiles help us not only to understand the role of the diverse variables involved, but also to design a biosensor of this kind. This figure does not show the most drastic concentration changes that occur just after the addition of the substrate. This is because the concentration profiles were saved every 20 s after the addition of the substrate. It is important to remember, however, that for t = 0 the values of C_S and C_P are equal to zero within the whole sensor.

All species show linear concentration profiles in the outer and inner membranes while concentration changes are particularly evidenced into the E-matrix, where the enzymatic reaction takes place. As a consequence of this, those profiles corresponding to the enzymatic product show maxima in the central region of the biosensor, Fig. 3B. This behavior evidences that the enzymatic product diffuses through both membranes to the electrode and to the bulk. On the contrary, concentration profiles of the mediator exhibit minima at the enzymatic matrix since this species is consumed by the enzyme and regenerated at the electrode surface, Fig. 3C. These results are in agreement with those of Gros et al., who studied the concentration of S, P and M species inside a film of 250 nm composed by polypyrrole and glucose oxidase [23]. They also found that, in spite of normal oxygen concentrations being around an order of magnitude lower than the physiological level of analytes like glucose, the use of mass-transport limiting films such as those presented in Fig. 1, tailors the flux of the substrate and O_2 [3,23].

The values of C_S and C_M into the sandwich are clearly not the same as those of the bulk. This difference is more significant for those cases where the value of v_{max} is high, Fig. 3A3–C3. It is well-known that mathematical expressions such as Eq. (4) or the Michaelis–Menten equation indicate the velocity of an enzymatic

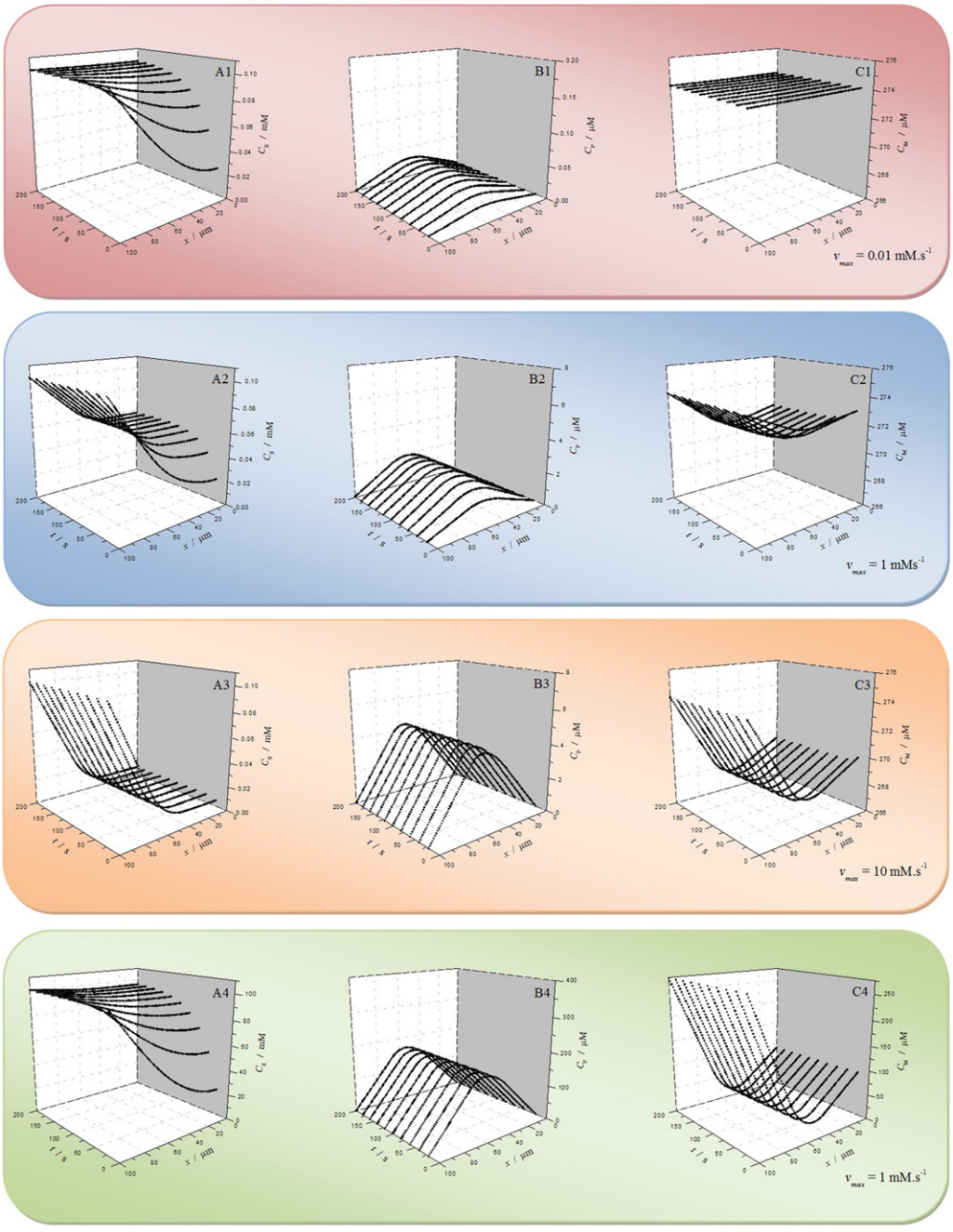

Fig. 3. Concentration profiles of (A) substrate, (B) product, and (C) mediator calculated as function of time and position within the membrane. The parameters used are: $C_M = 0.274$ mM, $D_S = 1 \times 10^{-6}$ cm^2 s^{-1}, $D_P = 5 \times 10^{-6}$ cm^2 s^{-1}, $D_M = 1 \times 10^{-5}$ cm^2 s^{-1}, $K_M = 7.1 \times 10^{-5}$ M, and $K_S = 2.2 \times 10^{-2}$ M. For (A1)–(C3) $C_S = 0.1$ mM, for (A4)–(C4) $C_S = 100$ mM, and on the right side of each group is v_{max}. The gray wall represents the electrode surface.

reaction. Nevertheless, it is worth to take in mind that these expressions involve values of C_S, C_E and C_M that would depend on the specific region of solution. For the case of an amperometric biosensor Eq. (4) refers to the concentration of these species into the enzymatic matrix, and not to their values in the bulk [19]. Some models assume high substrate concentrations to minimize the depletion of the substrate at the electrode surface. This assumption greatly simplifies the mathematical treatment of the problem, but, as it was pointed out by Bartlett et al., the resulting expression is valid only for certain restricted situations [22,37]. Moreover, approximated analytical solutions commonly use bulk concentrations instead of local concentrations. These solutions would particularly fail for systems with low values of C_S, where the Michaelis constant is estimated. In this regard, experiments have shown that substrate depletion should not be ignored, when there is either low substrate concentration and/or high enzyme activity [37].

From the analysis of these results it is clear that the performance of a sandwich-type biosensor of this kind cannot be described by simply considering the consumption of M, S, or the generation of P, since it is a function of several other parameters [9,38]. Although the concentrations of these species are related, it is necessary to evaluate the whole set of involved variables to provide a comprehensive description of the system [22]. This set of variables should entail the enzymatic constants as well as the concentrations and diffusion coefficients of species and particularly the thickness and/or

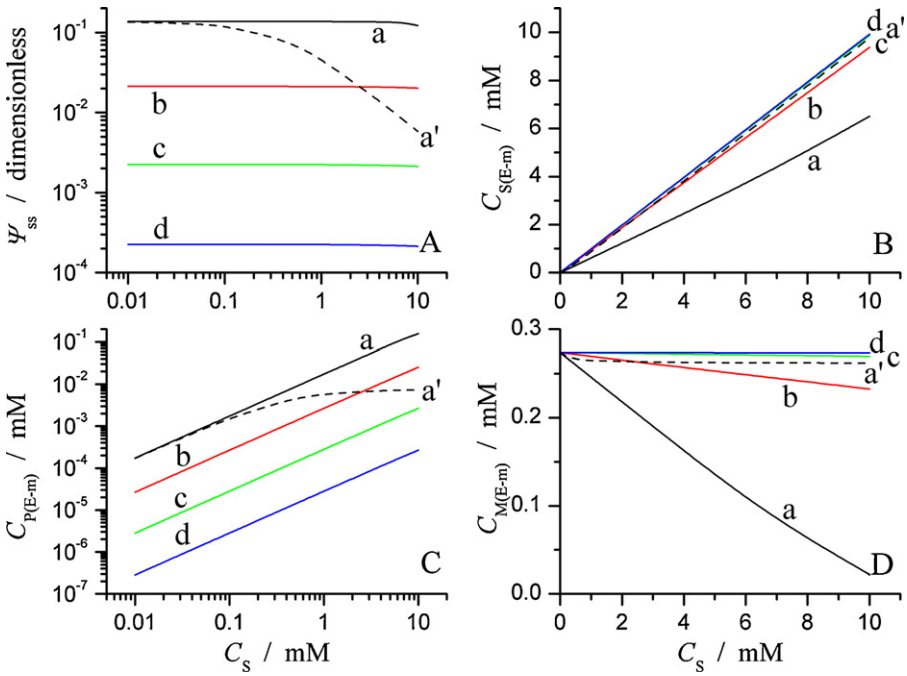

Fig. 4. Dependence of (A) Ψ_{ss} and of the average values that (B) C_S, (C) C_P and (D) C_M have within the enzymatic membrane as a function of C_S in the bulk. The parameters used are: $C_M = 0.274$ mM, $D_S = 1 \times 10^{-6}$ cm^2 s^{-1}, $D_P = 5 \times 10^{-6}$ cm^2 s^{-1}, $D_M = 1 \times 10^{-5}$ cm^2 s^{-1}, $K_S = 2.2 \times 10^{-2}$ M, $\Delta x = 100$ μm, $\delta t = 40$ ms, and different values of v_{max} (mM s^{-1}): (a) 10, (b) 1, (c) 0.1, (d) 0.01. Full lines: $K_M = 7.1 \times 10^{-5}$ M, dashed lines: $K_M = 2.2 \times 10^{-2}$ M.

dimensions of the biosensor. Thus, the higher consumption of the substrate in the enzymatic matrix is coupled to a proportional increase on the formation of the enzymatic product, Fig. 3B1–3. However, the concentration of O_2, the mediator, does not significantly change within the E-matrix, Fig. 3C1–3. On the one hand this is because O_2 is regenerated at the electrode surface and it diffuses much faster than the other involved species. On the other hand, this behavior does depend not only on the ratio between $C_S(D_S)^{1/2}$ and $C_M(D_M)^{1/2}$, but also on the constants K_M and K_S, since these parameters determine the amount of enzymatic product that can be generated for a given set of C_S and C_M.

Fig. 3C4 shows a situation in which the concentration of O_2 into the enzymatic membrane may be compromised. To achieve this, very high concentrations of substrate and values of v_{max} have been used. Even under these extreme conditions, the average concentration of the mediator in the E-matrix and in the inner membrane is still far of being zero. Besides, those devices that employ sandwich-type biomembranes commonly dilute the sample into a buffer. Thus, they are rarely exposed to solutions with very high values of C_S, directly.

Fig. 4 shows how Ψ_{ss} and the average values for C_S, C_P and C_M in the E-matrix depend on C_S. Different values of v_{max} and the effect of varying K_M have been also considered. As it is shown in Fig. 2, there is linear dependence between Ψ_{ss} and v_{max}. In other words, those biosensors with higher amount of enzyme will have higher sensitivity. Provided $K_M \ll K_S$, the value of Ψ_{ss} does not significantly change while C_S is increased. This indicates that the dimensional steady-state current can be linearly related to C_S, as it is typically intended for the case of a biosensor. However, if $K_M \approx K_S$, the current of this system may become limited by C_M, Fig. 4A(a′). The analysis of a biosensor with an enzyme presenting a ping-pong mechanism is usually simplified to be described by the Michaelis–Menten equation. This would be actually right when $1 \ll [K_S(C_S)^{-1}] \gg [K_M(C_M)^{-1}]$. Accordingly, the value of C_S from which the value of Ψ_{ss} starts to diminish depends on the ratios $K_S(C_S)^{-1}$ and $K_M(C_M)^{-1}$. For the case of $K_M = 2.2 \times 10^{-2}$ M, lower amounts of substrate and mediator are consumed, curves a′. However, also less concentration of product is being generated in the enzymatic membrane, Fig. 4C.

Fig. 5 presents dimensionless chronoamperometric transients calculated for a system in which the substrate would have different diffusion coefficients. This would correspond to a situation where outer membranes of different pore sizes are evaluated. As it can be observed, the sensitivity of the signal does not depend on D_S, but the response time does. In this regard, the reciprocal of the response time shows linear behavior as function of D_S. The linear dependence presented in the inset is not perfect because for the highest values of D_S the system becomes also controlled by the diffusion of the enzymatic product.

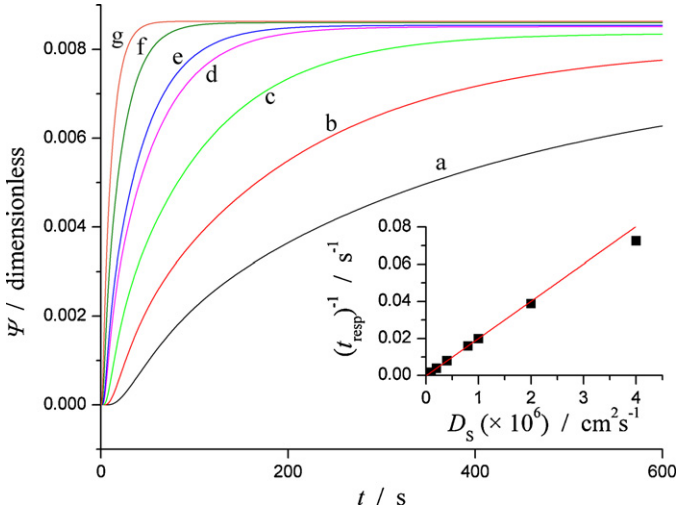

Fig. 5. Ψ–t transients calculated for: $D_P = 5 \times 10^{-6}$, $D_M = 1 \times 10^{-5}$, $K_M = 7.1 \times 10^{-5}$ M, $K_S = 2.2 \times 10^{-2}$ M, $v_{max} = 0.01$ mM s^{-1}, $\delta t = 40$ ms, $\Delta x = 100$ μm, $C_S = 1 \times 10^{-5}$ M, and D_S ($\times 10^7$ cm^2 s^{-1}) = (a) 1, (b) 2, (c) 4, (d) 8, (e) 10, (f) 20, (g) 40. *Inset*: Dependence of the reciprocal of t_{resp} on the value of D_S.

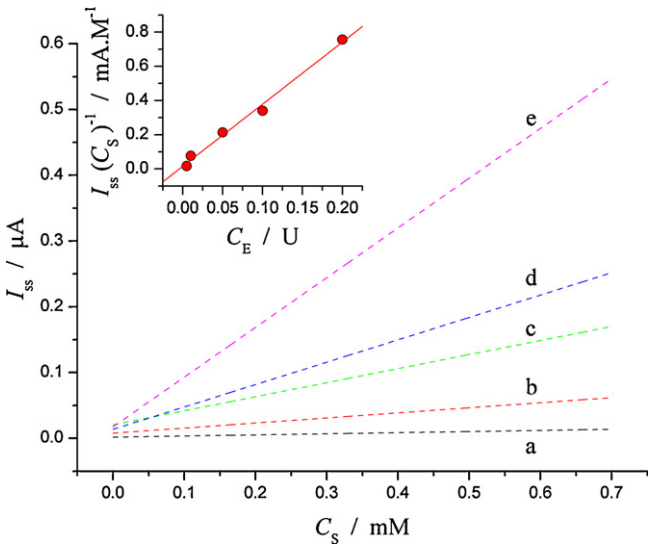

Fig. 6. Experimental calibration curves of lactate biosensors prepared with C_E (U): (a) 0.005, (b) 0.01, (c) 0.05, (d) 0.1, and (e) 0.2. The enzyme is LOD and the enzymatic product H_2O_2. E = 0.65 V, pH = 7.0. *Inset*: Dependence of the slope of calibration curves on C_E.

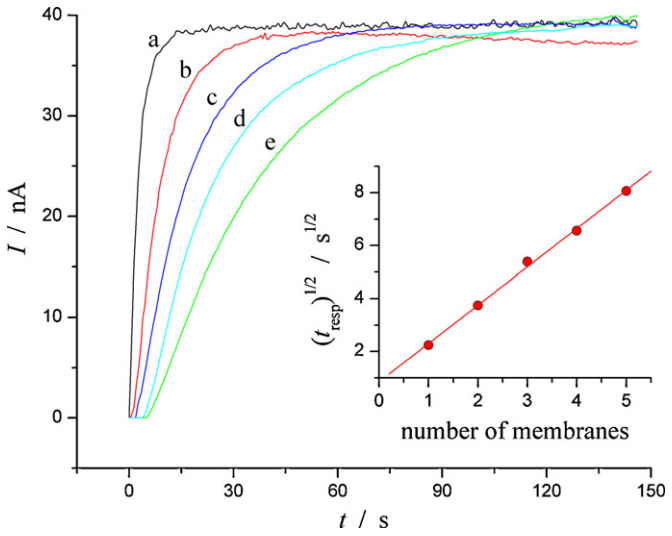

Fig. 7. Experimental chronoamperometric profiles for a set of lactate biosensors prepared with different number of external polycarbonate membranes. Sensors were prepared with 0.02 U of LOD and exposed to solutions of 100 μM lactate. Polycarbonate membranes have a 50 μm average pore size. *Inset*: Dependence of $(t_{resp})^{1/2}$ on the number of external membranes.

5. Comparison to experimental results

In this section, some characteristics calculated for the responses of sandwich-type biosensors are compared with experimental data. To evaluate the effect of v_{max} on the value of the steady-state current (I_{ss}), a set of calibration curves was performed for lactate biosensors prepared with different concentrations of enzyme, Fig. 6.

For these calibration curves, the enzyme was cross-linked by using glutaraldehyde according to the protocol described in Section 3. The unique difference is that diverse concentrations of LOD were used for each sensor. As it is shown, the slope of the calibration curves linearly increases with the amount of enzyme in the hydrogel. In other words, the sensitivity of the sensor is improved when more concentrated enzyme is used. The detection limit also improves with higher concentration of enzyme. However, the detection limit increases 3 times for a sensor with 20 times more concentrated enzyme. Bearing in mind that typical detection limits are around 1 μM, and that the basal level of lactate in blood is around 1 mM, it would not be necessary to use too much enzyme to provide a proper lactate biosensor [10,11].

These experimental outcomes are consistent with the theoretical results of Fig. 2. Nevertheless, the experimental dependence between amount of enzyme and I_{ss} would be lower than that predicted theoretically. This is because the model does not consider if there is a best mass ratio between the enzyme, hydrogel and cross-linker [10]. The lack of glutaraldehyde may result in the lost of the enzyme that was not properly linked to the matrix, while an excess of cross-linker could denature it [10]. Besides, simulated results do not consider effects such as the electrochemical active area or the ratio between diameters of the sandwich and the electrode.

Fig. 7 shows a set of chronoamperometric transients performed with a lactate biosensor in which, the number of external polycarbonate membranes is changed. After the addition of lactate all responses reached practically the same limiting current. A similar effect was observed in Fig. 5. In this case, however, the diffusion of the substrate has been controlled by varying the thickness of the external membrane. The relationship between the variables discussed in Figs. 5 and 7 could be summarized by the equation of diffusion: $\Delta x^2 = 2D_S t_{resp}$ [39]. As a result, the t_{resp} will be conditioned by the kind of external membrane that is chosen for a given biosensor. Thick membranes with small pore size will have higher t_{resp} than the thin membranes. This effect should not depend on the parameters of the enzymatic reaction.

6. Conclusions

A numerical model for the analysis of sandwich-type amperometric biosensors has been presented. The model considers the reaction of an oxidase enzyme that reacts according to a ping-pong mechanism in which H_2O_2 is generated. Although significant effort has been done for replacing O_2, the natural mediator, from a sample, this molecule would be more stable, naturally available, and with better kinetic and diffusive characteristics than any other proposed mediator. Perhaps because of this, the assay of glucose through enzyme-catalyzed reactions in which H_2O_2 is amperometrically measured has been the subject of more than 400 publications [1]. The use of mass-transport limiting films allows tailoring the flux of substrate and oxygen [3,4], while the effect of interference can be minimized by utilizing cation exchange or other permselective membranes [1,3,4].

According to the calculated curves, the concentration of reagents and products within the enzymatic matrix would rarely have the same value than in the bulk. In this regard, it is important to consider not only the concentration of involved species and the enzymatic constants, but also their diffusion coefficients and the dimensions of the biosensor.

Simulated profiles were compared with experimental data providing consistent results. In future publications the model will be integrated to a non-linear least squares fitting algorithm for estimating the parameters related to the chemical and geometrical aspects of diverse biosensors.

Acknowledgments

This work was funded by FONCYT, CONICET, and Secyt-UNC. F. Garay and A. Baruzzi are research fellows of CONICET.

References

[1] A. Heller, B. Feldman, Electrochemical glucose sensors and their applications in diabetes management, Chemical Reviews 108 (2008) 2482–2505.

[2] P.-C. Nien, P.-Y. Chen, K.-C. Ho, in: V.S. Somerset (Ed.), Intelligent and Biosensors, Vukovar, Croatia, 2010, pp. 245–268.
[3] J. Wang, Analytical Electrochemistry, 2nd edition, John Wiley & Sons, Inc., NY, USA, 2001.
[4] A. Mulchandani, K.R. Rogers, Enzymes and Microbial Biosensors: Techniques and Protocols, Humana Press Inc., NJ, USA, 1998.
[5] C. Dhand, M. Das, M. Datta, B.D. Malhotra, Recent advances in polyaniline based biosensors, Biosensors and Bioelectronics 26 (2011) 2811–2821.
[6] M.I. Prodromidis, M.I. Karayannis, Enzyme based amperometric biosensors for food analysis, Electroanalysis 14 (2002) 241–261.
[7] B.D. Malhotra, A. Chaubey, Biosensors for clinical diagnostics industry, Sensors and Actuators B 91 (2003) 117–127.
[8] S.R. Mikkelsen, E. Cortón, Bioanalytical Chemistry, John Wiley & Sons, Inc., NJ, USA, 2004.
[9] J. Wang, Glucose biosensors: 40 years of advances and challenges, Electroanalysis 13 (2001) 983–988.
[10] M.R. Romero, F. Garay, A. Baruzzi, Design and optimization of a lactate amperometric biosensor based on lactate oxidase cross-linked with polymeric matrixes, Sensors and Actuators B 131 (2008) 590–595.
[11] M.R. Romero, F. Ahumada, F. Garay, A. Baruzzi, Amperometric biosensor for direct blood lactate detection, Analytical Chemistry 82 (2010) 5568–5572.
[12] R. Krishnan, P. Atanasov, E. Wilkins, Mathematical modeling of an amperometric enzyme electrode based on a porous matrix of Stöber glass beads, Biosensors and Bioelectronics 11 (1996) 811–822.
[13] J.W. Parker, C.S. Schwartz, Modeling the kinetics of immobilized glucose oxidase, Biotechnology and Bioengineering 30 (1987) 724–735.
[14] S. Ghisla, V. Massey, Lactate oxidase, in: F. Müller (Ed.), Chemistry and Biochemistry of Flavoenzymes, vol. II, CRC Press, Boca Raton, USA, 1991, pp. 243–289.
[15] S.A.M. van Stroe-Biezen, A.P.M. Janssen, L.J.J. Janssen, A kinetic study of soluble glucose oxidase using a rotating-disc electrode, Bioelectrochemistry and Bioenergetics 33 (1994) 55–60.
[16] D.A. Gough, J.Y. Lucisano, P.H.S. Tse, Two-dimensional enzyme electrode sensor for glucose, Analytical Chemistry 57 (1985) 2351–2357.
[17] V. Flexer, K.F.E. Pratt, F. Garay, P.N. Bartlett, E.J. Calvo, Relaxation and simplex mathematical algorithms applied to the study of steady-state electrochemical responses of immobilized enzyme biosensors: comparison with experiments, Journal of Electroanalytical Chemistry 616 (2008) 87–98.
[18] A. Mattevi, To be or not to be an oxidase: challenging the oxygen reactivity of flavoenzymes, Trends in Biochemical Sciences 31 (2006) 276–283.
[19] V. Flexer, M.V. Ielmini, E.J. Calvo, P.N. Bartlett, Extracting kinetic parameters for homogeneous $[Os(bpy)_2ClPyCOOH]^+$ mediated enzyme reactions from cyclic voltammetry and simulations, Bioelectrochemistry 74 (2008) 201–209.
[20] I. Iliev, P. Atanasov, S. Gamburzev, A. Kaisheva, V. Tonchev, Transient response of electrochemical biosensors with asymmetrical sandwich membranes, Sensors and Actuators B 8 (1992) 65–72.
[21] K. Perauskas, R. Baronas, Computational modelling of biosensors with an outer perforated membrane, Nonlinear Analysis: Modeling and Control 14 (2009) 85–102.
[22] P.N. Bartlett, K.F.E. Pratt, Modelling of processes in enzyme electrodes, Biosensors and Bioelectronics 8 (1993) 451–462.
[23] P. Gros, A. Bergel, Improved model of a polypyrrole glucose oxidase modified electrode, Journal of Electroanalytical Chemistry 386 (1995) 65–73.
[24] A.A. Aziz, Mathematical modeling of an amperometric glucose sensor: the effect of membrane permeability and selectivity on performance, Jurnal Teknologi 51 (2009) 77–94.
[25] V. Rossokhaty, N. Rossokhata, Mathematical model of a biosensor with multilayer charged membrane, Computer Physics Communications 147 (2002) 366–369.
[26] A. Kartono, E. Sulistian, M. Mamat, The numerical analysis of enzyme membrane thickness on the response of amperometric biosensor, Applied Mathematical Science 4 (2010) 1299–1308.
[27] A. Bergel, M. Comtat, Theoretical evaluation of transient responses of an amperometric enzyme electrode, Analytical Chemistry 56 (1984) 2904–2909.
[28] S.W. Feldberg, in: J.S. Mattson, H.B. Mark, H.C. MacDonald (Eds.), Electrochemistry, Calculations, Simulations and Instrumentation, vol. 2, Marcel Dekker, New York, 1972.
[29] F. Garay, C.A. Barbero, Charge neutralization process of mobile species at any distance from the electrode/solution interface. 1. Theory and simulation of concentration and concentration gradients developed during potentiostatic conditions, Analytical Chemistry 78 (2006) 6733–6739.
[30] F. Garay, C.A. Barbero, Charge neutralization process of mobile species developed during potentiodynamic conditions. Part 1. Theory, Journal of Electroanalytical Chemistry 624 (2008) 218–227.
[31] S.B. Hall, E.A. Khudaish, A.L. Hart, Electrochemical oxidation of hydrogen peroxide at platinum electrodes. Part 1. An adsorption-controlled mechanism, Electrochimica Acta 43 (1997) 579–588.
[32] S.B. Hall, E.A. Khudaish, A.L. Hart, Electrochemical oxidation of hydrogen peroxide at platinum electrodes. Part II. Effect of potential, Electrochimica Acta 43 (1998) 2015–2024.
[33] F. Garay, C.A. Barbero, Charge neutralization process of mobile species at any distance from the electrode/solution interface. 2. Concentration gradients during potential pulse experiments, Analytical Chemistry 78 (2006) 6740–6746.
[34] F. Garay, R.A. Iglesias, C.A. Barbero, Charge neutralization process of mobile species developed during potentiodynamic conditions. Part 2. Simulation and fit of probe beam deflection experiments, Journal of Electroanalytical Chemistry 624 (2008) 211–217.
[35] H. Li, R. Luo, Modeling and characterization of glucose-sensitive hydrogel: effect of Young's modulus, Biosensors and Bioelectronics 24 (2009) 3630–3636.
[36] B. Csóka, B. Kovács, G. Nagy, Investigation of concentration profiles inside operating biocatalytic sensors with scanning electrochemical microscopy (SECM), Biosensors and Bioelectronics 18 (2003) 141–149.
[37] P.N. Bartlett, K.F.E. Pratt, A study of the kinetics of the reaction between ferrocene monocarboxylic acid and glucose oxidase using the rotating-disc electrode, Journal of Electroanalytical Chemistry 397 (1995) 53–60.
[38] C.G.J. Koopal, R.J.M. Nolte, Kinetic study of the performance of third-generation biosensors, Bioelectrochemistry and Bioenergetics 33 (1994) 45–53.
[39] A.J. Bard, L.R. Faulkner, Electrochemical Methods: Fundamentals and Applications, 2nd edition, John Wiley & Sons, Inc., New York, USA, 2001.

Biographies

Marcelo Ricardo Romero, Doctor (Universidad Nacional de Córdoba, 2011). Currently he is a postdoctoral researcher at the Department of Organic Chemistry, School of Chemical Science, Universidad Nacional de Córdoba. His fields of interest include electrochemistry, analytical chemistry, polymer science, electronic devices and biosensors.

Ana M. Baruzzi, Doctor (Universidad Nacional de Córdoba, 1981). Currently she is a full professor at the Department of Physical Chemistry, School of Chemical Science, Universidad Nacional de Córdoba and research fellow of CONICET, Argentina. Her fields of interest include electrochemistry, analytical chemistry, polymer science and biosensors.

Fernando Garay, Doctor (Universidad Nacional de Córdoba, 2002). Currently he is an assistant professor at the Department of Physical Chemistry, School of Chemical Science, Universidad Nacional de Córdoba and research fellow of CONICET, Argentina. His fields of interest include electrochemistry, numerical and digital simulations, analytical chemistry, in situ techniques, polymer science and biosensors.